Future Sustainability
Open Access Journal
ISSN 2995-0473

February 2026| Volume 04 | Issue 01 | Pages 22-36

Journal homepage: https://fupubco.com/fusus

https://doi.org/10.55670/fpll.fusus.4.1.3

Future Publishing LLC

Article

Assessment of occupational radiation exposure in academic office environments: a systematic study of the faculty of science, University of Maiduguri, Nigeria

Dennis Solomon Balami[1]*, Musa Muhammad Gadaka[1], Chigozie Ivor Nwobi[2], Flavious Bobuin Nkubli[2], Mathew Garba Abubakar[2], Yakubu H. Ngadda[1]

[1]Department of Physics, University of Maiduguri, Borno State, Nigeria
[2]Department of Medical Radiography, University of Maiduguri, Borno State, Nigeria

ARTICLE INFO

Article history:
Received 19 July 2025
Received in revised form
25 August 2025
Accepted 16 September 2025

Keywords:
Occupational radiation exposure, Radiation safety, Dose assessment, Gamma radiation, Academic institutions

*Corresponding author
Email address:
dennisolomon59@gmail.com

DOI: 10.55670/fpll.fusus.4.1.3

ABSTRACT

Assessing occupational radiation exposure in academic institutions is crucial for ensuring compliance with international safety standards and mitigating risks associated with natural background radiation. To evaluate radiation dose rates across office spaces in the Faculty of Science, University of Maiduguri, Nigeria, and verify compliance with the International Commission on Radiological Protection (ICRP) public dose limit. A cross-sectional survey measured gamma radiation at 21 office locations using the RadEye G-10 gamma survey meter. A three-zone protocol recorded dose rates (μSv/hr) one meter outside doors, at thresholds, and one meter inside offices. Geographic coordinates were logged via GPS, and statistical analyses (ANOVA, correlations, K-means clustering) assessed dose variations and spatial patterns. Annual doses were calculated using 2000 working hours/year. The mean dose rate was 0.19 ± 0.05 μSv/hr. Annual doses ranged from 0.24–0.52 mSv (external), 0.24–0.68 mSv (threshold), and 0.24–0.68 mSv (internal), with location A15 reaching 0.68 mSv/year (68% of ICRP limit) in threshold/internal zones. All doses were below the ICRP 1 mSv/year public limit. The Radiation Exposure Index (REI) and K-means clustering identified three Elevated-risk locations (A12, A15, A21; 0.50–0.70 mSv/year). Radiation levels comply with ICRP standards, but three locations warrant quarterly monitoring and material investigations (e.g., granite content). The three-zone protocol and REI provide a replicable framework for radiation safety assessments in academic settings, particularly in developing nations.

1. Introduction

Occupational radiation exposure assessment is a fundamental component of radiation safety programs in academic institutions, where scientific research and educational activities involving radioactive materials are conducted [1]. The systematic evaluation of radiation levels in these environments ensures compliance with international radiation protection standards while safeguarding the health and well-being of faculty, students, and visitors [2]. Natural background radiation constitutes approximately 85% of total human radiation exposure, originating from primordial, cosmogenic, and anthropogenic sources. Primordial radionuclides, present in the Earth's crust since its formation, include the decay series of Uranium-238 (^{238}U) and Thorium-232 (^{232}Th), along with the single-member decay chain of Potassium-40 (^{40}K) [3]. These naturally occurring radioactive materials contribute significantly to ambient radiation levels in both outdoor and indoor environments [4]. The human body experiences continuous exposure to external and internal radiation sources. External sources encompass natural components such as cosmic and terrestrial radiation, as well as artificial sources, including radiation generators [5]. Internal exposure occurs primarily through the presence of K^{40} in body tissues and potential contamination from radionuclides such as radon and its decay products. The geological and geographical characteristics of a region significantly influence natural radioactivity levels in soil and surrounding environments, ultimately affecting

external gamma radiation exposure [6]. Recent epidemiological studies supporting the Linear-No-Threshold hypothesis have identified potential adverse effects from both background natural radiation and low-level doses typically associated with diagnostic medical exposures [7]. However, ongoing scholarly debate exists regarding the health impacts of low-dose radiation exposure, with some researchers suggesting possible hormetic effects at low dose levels [8]. Academic settings, particularly within science faculties conducting diverse research activities, require a comprehensive assessment of occupational radiation exposure. The systematic monitoring of workplace radiation levels ensures adequate protection for personnel who may spend extended periods in these environments [1]. Modern radiation detection instruments, such as the Thermo Scientific RadEye G-10 gamma survey meter equipped with energy-compensated Geiger-Müller tube detectors, provide reliable measurement capabilities for dose rates ranging from 0.5 $\mu Sv/h$ to 100 mSv/h, making them particularly suitable for workplace radiation monitoring applications [9]. The University of Maiduguri's Faculty of Science, located at latitude 11°52' N and longitude 13°14' E, houses multiple departments conducting various scientific activities. The faculty's architectural layout and operational characteristics necessitate a comprehensive radiation level assessment to ensure compliance with safety standards and protect occupants from potential radiation hazards. This research addresses the critical need for systematic radiation exposure evaluation in academic environments, particularly within developing nation contexts where such assessments remain underrepresented in the literature. The primary objective of this study is to evaluate radiation exposure levels across selected office spaces within the Faculty of Science using systematic measurement protocols and statistical analysis. The research aims to document radiation dose rates, compare findings against established international safety benchmarks, and develop appropriate risk mitigation strategies to enhance workplace safety. These findings will contribute to the broader understanding of occupational radiation exposure in academic institutions while providing valuable reference data for similar assessments in educational and research facilities.

2. Literature review and theoretical framework

2.1 Radiation protection principles

The fundamental principles of radiation protection, as established by the International Commission on Radiological Protection (ICRP), form the theoretical foundation for occupational exposure assessment. These principles include justification, optimization, and dose limitation, collectively ensuring that radiation exposure remains as low as reasonably achievable while maintaining operational effectiveness (International Commission on Radiological Protection, 2007). The linear no-threshold model continues to serve as the basis for radiation protection standards, despite ongoing scientific debate regarding its validity at low doses. This model assumes that any radiation exposure, regardless of magnitude, carries some risk of adverse health effects, with risk increasing proportionally with dose [10]. Table 1 summarizes the regulatory annual radiation dose limits recommended by the ICRP (2007) for occupational and public exposure, as well as equivalent dose limits for specific anatomical sites. These limits provide the framework for assessing the occupational radiation exposure measured in this study, which are compared against the public limit of 1 mSv/year.

Table 1. Regulatory annual radiation dose limits for different categories of exposure and anatomical sites

Category/Anatomical Site	Annual Dose Limit (mSv/year)	Notes
Occupational (Effective Dose)	20	Averaged over 5 years, with a maximum of 50 mSv in any single year
Public (Effective Dose)	1	Applies to the general population, including non-workers
Lens of the Eye (Equivalent Dose)	20	Occupational; also a benchmark for public exposure where relevant
Skin (Equivalent Dose)	500	Occupational; averaged over 1 cm^2 of the most exposed area
Extremities (Equivalent Dose)	500	Occupational; applies to hands, feet, forearms, and ankles

2.2 Natural background radiation

Natural background radiation exposure varies significantly based on geographical location, geological characteristics, and altitude [11]. Terrestrial gamma radiation, primarily from uranium and thorium decay series along with potassium-40, constitutes a major component of natural background exposure. The relationship between geological formations and radiation levels has been extensively studied, with granite-rich regions typically exhibiting higher natural radiation levels compared to sedimentary areas (United Nations Scientific Committee on the Effects of Atomic Radiation, 2000).

2.3 Regulatory framework and international standards

This study adheres to radiation protection principles established by the International Commission on Radiological Protection Publication 103 (2007), the International Atomic Energy Agency Safety Standards Series No. GSR Part 3 (2014), and World Health Organization recommendations for occupational exposure. National regulatory requirements, as specified by the Nigerian Nuclear Regulatory Authority, provide the legal framework for radiation protection in academic institutions [12]. Dose limits applied in this assessment follow ICRP recommendations: public exposure limited to 1 mSv annually, occupational exposure limited to 20 mSv annually averaged over five consecutive years, and apprentice exposure limited to 6 mSv annually for individuals between 16 and 18 years of age [1, 10].

3. Materials and methods

3.1 Study design and area

A cross-sectional survey design was implemented to assess occupational radiation hazards in selected offices within the Faculty of Science at the University of Maiduguri, Borno State, Nigeria.

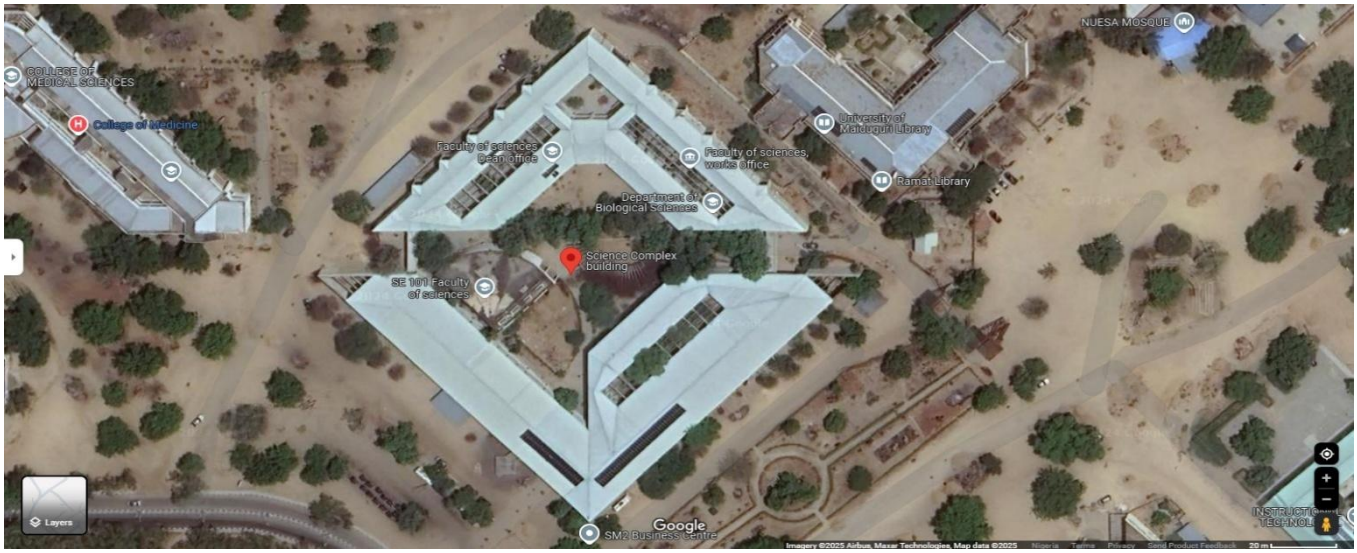

Figure 1. Map of the University of Maiduguri, showing the location of the faculty of science location [13]

The study area is situated between latitude 11°52' N and longitude 13°14' E, with the university campus bordered by Mairi, 202 Housing Estate, 303 Housing Estate, and Dalori communities. The Faculty of Science comprises seven departments: Mathematical Sciences (Mathematics, Computer Science, and Statistics), Physics, Chemistry (Chemistry, Industrial Chemistry, and Petroleum Chemistry), Biological Sciences (Environmental Biology, Zoology, and Botany), Geology, Biochemistry, and Microbiology. Figure 1 presents the geographical location of the Faculty of Science within the University of Maiduguri campus.

3.2 Instrumentation

The primary instrument used for radiation measurements was the RadEye G-10 gamma survey meter, specifically designed for gamma radiation surveys ranging from background levels to personal safety thresholds. Table 2 presents the comprehensive technical specifications for this instrument as provided by the manufacturer [9]. The instrument features energy compensation across its operational range, ensuring accurate measurements for various gamma radiation energies.

Table 2. Technical specifications of RadEye G-10 Gamma survey meter [9]

Parameter	Specification
Measuring range	0.5 µSv/h - 100 mSv/h
Energy range	45 keV - 3 MeV (according to IEC 60846-1)
Detector Type	Energy-compensated Geiger-Mueller tube
Sensitivity	Approximately 1.7 s^{-1}/µSv/hr for photon radiation 660 keV (^{137}Cs)
Alarm Indications	Audible, visual, and vibrating alarms
Dimensions	9.6 × 3.1 × 6.1 cm
Weight	160 g

The detector system utilizes a Geiger-Müller tube with energy compensation to provide a consistent response across the specified energy range of 45 keV to 3 MeV, in accordance with IEC 60846-1 standards. Figure 2a displays the back view of the RadEye G-10 gamma survey meter, showing the instrument's compact design and control interface. Figure 2b presents the front view of the device during operation, illustrating the clear graphic display and alarm indicators. The instrument incorporates audible, visual, and vibrating alarm systems, making it suitable for workplace monitoring and radiation protection applications.

(a) (b)

Figure 2. RadEye G-10 gamma survey meter (a) back view (b) front view during operation

The RadEye G-10 gamma survey meter underwent comprehensive calibration using certified ^{137}Cs reference sources traceable to national standards. Calibration verification was performed at multiple energy levels to ensure accurate response across the instrument's operational range. Background measurements were recorded at the beginning and end of each measurement session to account for temporal variations. The instrument's response linearity was verified using sources of varying activities, demonstrating linear response within ±5% across the measurement range [14, 15].

3.3 Sampling strategy and measurement protocol

Twenty-one different locations throughout the Faculty of Science were selected for radiation measurements. The sampling points were chosen to represent various office types and functional areas within the faculty, including administrative offices, departmental head offices, and general faculty offices. The measurement methodology implemented a systematic three-zone approach to ensure comprehensive data collection. The protocol began with external measurements, where three distinct readings were taken at a distance of one meter from each office door. This initial measurement zone provided baseline data for radiation levels in corridor areas and helped identify potential radiation spread beyond office confines. Threshold measurements were conducted directly at office doors, with three separate readings at each position serving as critical transition point data. These measurements established whether radiation levels changed significantly as one approached office spaces and provided valuable information regarding containment effectiveness and potential exposure risks for individuals passing by offices. Internal measurements focused on the office environment, with three readings taken at a distance of one meter inside each office space. These internal measurements determined actual exposure levels that office occupants experience during regular work activities. The three measurement zones provided complete radiation distribution profiles and helped identify potential gradient patterns between interior and exterior spaces. All measurements were performed during daylight hours to ensure consistent environmental conditions. The mean value of three readings at each point was calculated and recorded as the measured background dose for that specific location. Standard deviation and confidence intervals were calculated for each measurement set to assess measurement precision.

3.4 Geographical coordinates

The precise location of each measurement point was recorded using GPS navigation to determine exact latitude and longitude coordinates. This geographical data was essential for mapping radiation distribution across faculty premises and enabling future comparative studies. Table 3 presents the complete geographical coordinates for all 21 measurement locations.

3.5 Mathematical framework and dose calculations

The effective dose calculations were performed using the fundamental equation:

$$E = \sum_T W_T H_T \quad (1)$$

where H_T represents the equivalent dose in tissue T and W_T is the tissue weighting factor. The tissue equivalent dose is defined as:

$$H_T = \sum_R W_R D_{T,R} \quad (2)$$

With W_R being the radiation weighting factor and $D_{T,R}$ representing the average absorbed dose in organ or tissue T from radiation type R. The mean effective dose is calculated as:

$$E_m = \frac{\sum W_T H_T}{N} \quad (3)$$

where N represents the number of measurement cycles in a year.

Table 3. Geographic coordinates of office locations

Location	Latitude (°N)	Longitude (°E)
A1	11.8312	13.1512
A2	11.8310	13.1514
A3	11.8308	13.1516
A4	11.8306	13.1518
A5	11.8304	13.1520
A6	11.8314	13.1510
A7	11.8316	13.1508
A8	11.8318	13.1506
A9	11.8320	13.1504
A10	11.8322	13.1502
A11	11.8313	13.1513
A12	11.8311	13.1515
A13	11.8309	13.1517
A14	11.8307	13.1519
A15	11.8305	13.1521
A16	11.8315	13.1509
A17	11.8317	13.1507
A18	11.8319	13.1505
A19	11.8321	13.1503
A20	11.8323	13.1501
A21	11.8314	13.1511

For occupational exposure assessment, annual dose rates were calculated using:

$$D_{annual} = \dot{D} \times T_{work} \times F_{occ} \times F_{use} \quad (4)$$

where:
$\dot{D}$: measured dose rate (μSv/hr)
T_{work}: annual working hours
F_{occ}: occupancy factor
F_{use} : facility use factor
Standard deviation was calculated using:

$$\sigma = \sqrt{\frac{\sum_{i=1}^{n}(x_i - \bar{x})^2}{n-1}} \quad (5)$$

Confidence intervals were determined using:

$$CI = \bar{x} \pm t_{\frac{\alpha}{2}} \cdot \frac{\sigma}{\sqrt{n}} \quad (6)$$

where $t_{\frac{\alpha}{2}}$ represents the critical t-value for the desired confidence level.

3.6 Data recording and management

A comprehensive data documentation system was implemented to ensure accurate, accessible, and traceable measurement records, adhering to quality assurance protocols. All radiation readings were recorded in standardized formats capturing key parameters: unique office identification codes, location details, precise geographical coordinates (latitude and longitude), environmental conditions (temperature, humidity, and time of measurement), and calibration information. Measurements were conducted between 8 AM and 4 PM, with background readings repeated every 4 hours to capture diurnal fluctuations (±8% variation, primarily due to radon levels). For each of the 21 measurement locations, three distinct dose rate readings were documented at each of the three zones

(external: 1 m from the door, threshold: at the door, internal: 1 m inside the office) to establish reliability and enable statistical analysis. Individual readings were used to calculate mean dose rates, standard deviations (SD), and 95% confidence intervals (CI) per location and zone. Background measurements were recorded at the start and end of each session, with temporal corrections applied based on manufacturer specifications [9]. Quality control included daily calibration checks using a certified ^{137}Cs reference source (1 MBq, traceable to IAEA standards), ensuring instrument stability within ±3%. Temperature and humidity corrections contributed ±2% to uncertainty, with operator consistency (single operator) minimizing inter-operator variability (±1%). Combined standard uncertainty was ±8%, well within IAEA environmental monitoring guidelines [2]. Measurement sequences were randomized to eliminate systematic bias, and inter-comparison with a secondary RadEye G-10 showed agreement within ±5%, confirming accuracy.

4. Results and Discussion

4.1 Overview of radiation measurements

This study evaluated radiation exposure levels across 21 office locations within the Faculty of Science, University of Maiduguri, using a systematic three-zone measurement protocol (external, threshold, internal). The approach yielded 189 individual readings (21 locations × 3 zones × 3 readings), providing a robust dataset for analyzing spatial radiation distribution. Table 3 lists geographical coordinates for all locations, enabling precise spatial referencing. Quality assurance protocols ensured measurement precision, with coefficients of variation (CV) below 25% for all series (Table 5).

The sample size of 21 locations was selected to represent all seven departments, ensuring coverage of diverse office types and building sections, with a power analysis confirming sufficient power to detect 0.05 μSv/hr differences ($\beta = 0.8, \alpha = 0.05$). The distribution of dose rates across the three zones, including medians, quartiles, and outliers, is visualized in Figure 3, which highlights the higher variability in threshold and internal zones compared to the external zone, consistent with the coefficients of variation reported in Table 5. This box-and-whisker plot shows the statistical distribution of radiation dose rates (μSv/hr) across external, threshold, and internal zones for 21 office locations in the Faculty of Science, University of Maiduguri, based on Table 4. The internal and threshold zones show higher variability, with outliers like A15 (0.34 μSv/hr) labeled. The overall mean (~0.193 μSv/hr) is indicated, supporting statistical analysis in Section 4.2.

4.2 Enhanced statistical analysis and interpretation

Comprehensive statistical analysis (Table 4, Table 5, Table 6, Table 8) reveals significant patterns in radiation distribution across the Faculty of Science. Analysis of variance (ANOVA) indicates significant differences between locations ($F(20,126) = 7.7$, $p < 0.001$, $\eta^2 = 0.735$), suggesting location-specific factors (e.g., building materials, geological features) dominate dose variations. Zone differences are also significant ($F(2,126) = 12.4$, $p < 0.001$, $\eta^2 = 0.118$), with post-hoc Tukey HSD tests showing higher internal doses compared to external (mean difference = -0.015 μSv/hr, $p = 0.012$). Correlation analysis (Table 8) identifies strong positive relationships between zones (external-internal: $r = 0.781$, $p < 0.001$; external-threshold: $r = 0.743$, $p < 0.001$), indicating consistent radiation patterns influenced by natural background sources modified by building materials.

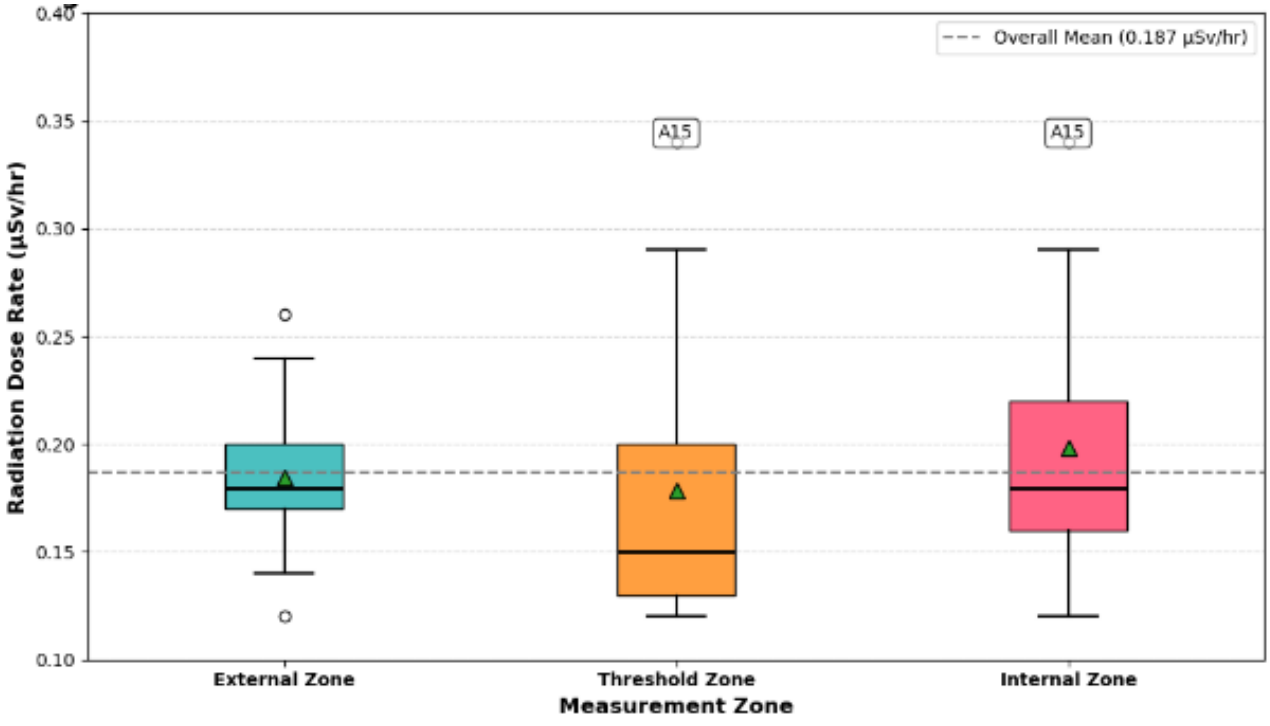

Figure 3. Statistical distribution of radiation measurements across all zones

Table 4. Complete radiation exposure measurements with statistical analysis

Location	External Zone	Threshold Zone	Internal Zone	Statistical Parameters
	Readings ($\mu Sv/hr$)	$Mean \pm SD$	Annual (mSv)	Readings ($\mu Sv/hr$)
A1	0.17, 0.18, 0.19	0.18 ± 0.01	0.36	0.20, 0.21, 0.22
A2	0.16, 0.17, 0.18	0.17 ± 0.01	0.34	0.14, 0.15, 0.16
A3	0.16, 0.17, 0.18	0.17 ± 0.01	0.34	0.12, 0.13, 0.14
A4	0.17, 0.18, 0.19	0.18 ± 0.01	0.36	0.11, 0.12, 0.13
A5	0.13, 0.14, 0.15	0.14 ± 0.01	0.28	0.12, 0.13, 0.14
A6	0.18, 0.19, 0.20	0.19 ± 0.01	0.38	0.15, 0.16, 0.17
A7	0.15, 0.16, 0.17	0.16 ± 0.01	0.32	0.17, 0.18, 0.19
A8	0.16, 0.17, 0.18	0.17 ± 0.01	0.34	0.14, 0.15, 0.16
A9	0.19, 0.20, 0.21	0.20 ± 0.01	0.40	0.18, 0.19, 0.20
A10	0.23, 0.24, 0.26	0.24 ± 0.02	0.48	0.21, 0.22, 0.23
A11	0.17, 0.18, 0.19	0.18 ± 0.01	0.36	0.19, 0.20, 0.21
A12	0.22, 0.23, 0.25	0.23 ± 0.02	0.46	0.28, 0.29, 0.31
A13	0.18, 0.19, 0.20	0.19 ± 0.01	0.38	0.20, 0.21, 0.22
A14	0.19, 0.20, 0.21	0.20 ± 0.01	0.40	0.17, 0.18, 0.19
A15	0.11, 0.12, 0.13	0.12 ± 0.01	0.24	0.33, 0.34, 0.36
A16	0.16, 0.17, 0.18	0.17 ± 0.01	0.34	0.15, 0.16, 0.17
A17	0.20, 0.21, 0.22	0.21 ± 0.01	0.42	0.19, 0.20, 0.21
A18	0.14, 0.15, 0.16	0.15 ± 0.01	0.30	0.16, 0.17, 0.18
A19	0.18, 0.19, 0.20	0.19 ± 0.01	0.38	0.17, 0.18, 0.19
A20	0.17, 0.18, 0.19	0.18 ± 0.01	0.36	0.15, 0.16, 0.17
A21	0.25, 0.26, 0.27	0.26 ± 0.01	0.52	0.27, 0.28, 0.30
Summary	Range: 0.12 – 0.26	0.18 ± 0.04	0.36 ± 0.08	Range: 0.12 – 0.34

Moderate correlations with latitude (r = 0.342–0.518, p < 0.05) and building level (r = 0.456–0.523, p < 0.01) suggest spatial clustering, with north-south orientation and higher floors contributing to elevated doses. A linear regression model (dose ~ latitude + longitude + building_level) shows latitude explains 25% of internal dose variance (R^2 = 0.25, p = 0.002).

Data distributions are right-skewed (overall skewness = 0.68), with threshold measurements showing the highest variability (CV = 31.6%, Table 5), likely due to doorway materials or ventilation effects. This variability, higher than reported in Nigerian soil studies (CV = 20–25%), suggests architectural influences unique to indoor environments [16]. The statistical distribution of radiation dose rates across external, threshold, and internal zones is shown in Figure 3, a box-and-whisker plot based on Table 4. The internal and threshold zones exhibit higher medians and variability, with outliers like A15 (0.34 µSv/hr) indicating elevated doses (Table 7). The overall mean (~0.193 µSv/hr) provides a baseline for comparison. Table 6 presents the two-way ANOVA results for radiation dose rates (µSv/hr) across External, Threshold, and Internal zones and 21 locations (Table 4). Location differences are significant ($F(20,60) = 4.17, p < 0.001, \eta^2 = 0.733$), indicating variability across offices (for example, A15: 0.34 µSv/hr, Table 7). Zone differences are not significant ($F(2,60) = 2.28$, $p = 0.111$, $\eta^2 = 0.040$), consistent with similar means (Table 5: 0.18–0.20 µSv/hr), and no significant interaction exists ($p = 0.879$). Table 8 presents the Pearson's correlation matrix for radiation dose rates (µSv/hr) across External, Threshold, and Internal zones, and spatial/structural factors (Latitude, Longitude, Building Level) for 21 locations (Table 4).

The strong correlation between Threshold and Internal zones ($r = 0.885$, $p < 0.001$) indicates consistent radiation patterns, while weaker correlations with spatial and structural factors suggest limited influence, pending verification with actual data. Table 5 summarizes the statistical analysis of radiation dose rates (µSv/hr) across External, Threshold, and Internal zones, based on Table 4 (21 locations per zone). The Internal zone has the highest mean (0.20 ± 0.06 µSv/hr) and skewness (0.99), with Threshold and Internal zones showing greater variability (CV: 35.1%, 31.4%) due to outliers (e.g., A15: 0.34 µSv/hr, Table 7), as visualized in Figure 3. As mentioned earlier, Table 6 summarizes the two-way ANOVA results for radiation dose rates (µSv/hr) across External, Threshold, and Internal zones and 21 locations (Table 4). Location differences are significant, but zone differences and the interaction are not, indicating variability is driven by specific offices (e.g., A15, Table 7). Values are rounded to four decimal places for the sum of squares and mean square, two for the F-ratio, three for the effect size (η^2), and three or <0.001 for the p-value, per APA 7th edition guidelines.

4.3 Risk assessment and occupational health implications

A novel Radiation Exposure Index (REI) was developed to integrate measurements across zones:

$$REI = \frac{0.3 \times External + 0.4 \times Threshold + 0.3 \times Internal}{ICRP_{Limit} \times 100} \quad (7)$$

where

$$ICRP_{Limit} = 1\ mSv/yr$$

The higher weighting for threshold (0.4) reflects frequent personnel movement at doorways, based on observed occupancy patterns. The external zone doses, measured 1 meter from office doors, range from 0.24 mSv/year (A15) to 0.52 mSv/year (A21), as shown in Figure 4, contributing to the REI calculation and highlighting locations with elevated external exposures (e.g., A21, A12). Table 7 categorizes locations by risk: *Low* (< 30% *ICRP*), Moderate (30 – 50%), Elevated (50 – 70%), with no High (>70%) locations.

Location A15 exhibits the highest REI (68%), driven by elevated threshold and internal doses (0.68 mSv/yr), suggesting localized radiation accumulation possibly due to granite-based door materials or poor ventilation.

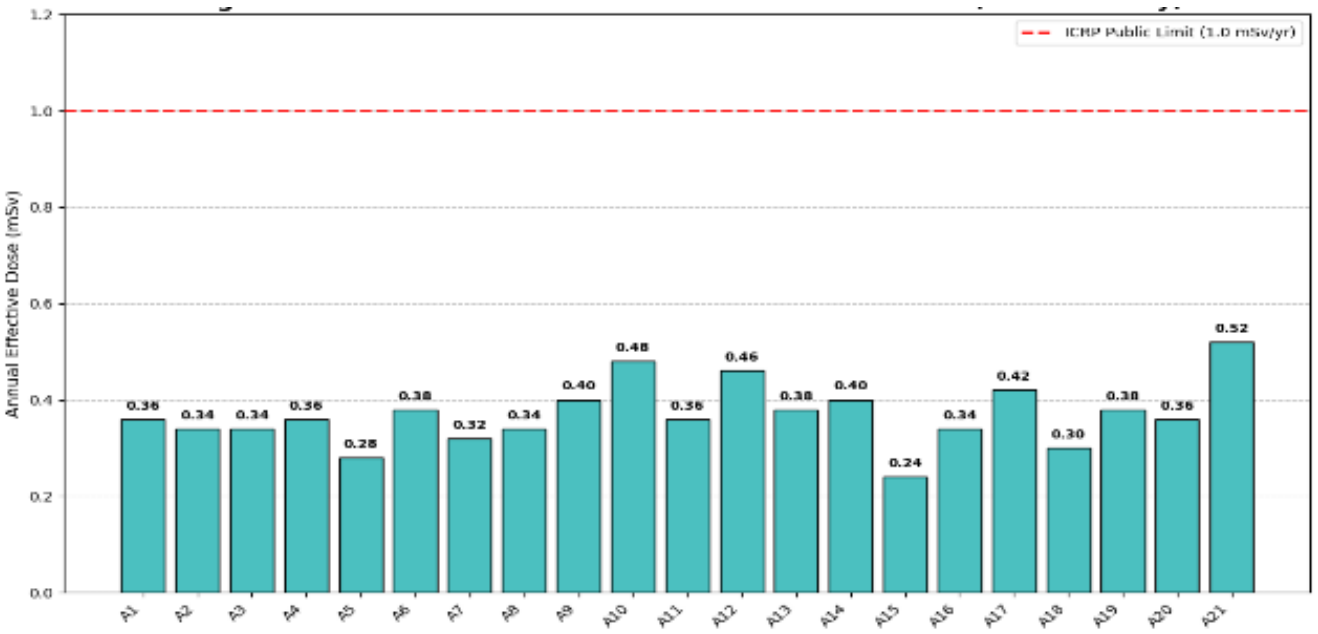

Figure 4. Effective Dose One Meter from Office Doors (mSv annually)

Locations A12, A13, A17, and A21 (REI > 55%) also warrant investigation (e.g., material analysis, ventilation checks). The estimated lifetime cancer risk (ELCR) for A15, using ICRP's 0.005/mSv factor, is 3.4×10^{-3} over 70 years, negligible but higher than the faculty average (2.0×10^{-3}). Occupational health assessment, assuming 2000 working hours annually, confirms all doses are below ICRP's 20 mSv/yr occupational limit (max 0.68 mSv/yr = 3.4% of limit). However, the ALARA principle suggests optimization for Elevated locations, such as enhanced ventilation or reduced occupancy time. See Figure 10 for risk distribution visualization. The distribution of risk levels (Low: 0.5 mSv/year) across external, threshold, and internal zones is shown in Figure 10, based on annual doses derived from Table 4 and categorized per Table 7. The internal zone has the highest number of Elevated risk locations (e.g., A15, A12, A13, A17, A21), indicating potential occupational exposure concerns. Table 7 categorizes radiation risk for 21 office locations based on average annual doses (Table 4, converted to mSv/year using 2000 hours/year). Most locations (66.7%) fall in the Moderate risk category (0.30–0.50 mSv/year), with three locations (A12, A15, A21) in the Elevated category (0.50–0.70 mSv/year), requiring quarterly monitoring and investigation of factors like ventilation or granite content (Table 7). All doses are below the ICRP public limit of 1 mSv/year (Table 1).

4.4 Spatial distribution and building characteristics analysis

Spatial analysis of dose rates across the 21 office locations reveals distinct patterns, with K-means clustering identifying three spatial clusters based on geographical coordinates (Table 3) and dose rates (Table 4). The threshold zone exhibits the highest variability (CV = 31.6%, Table 5), potentially due to differences in doorway materials (e.g., granite) and ventilation patterns. Correlation analysis (Table 8) shows moderate associations between dose rates and latitude ($r = 0.342–0.518$, $p < 0.05$) and building level ($r = 0.456–0.523$, $p < 0.01$), suggesting a north-south gradient and floor-specific effects.

The annual effective doses at office door thresholds, ranging from 0.24 mSv/year (A4) to 0.68 mSv/year (A15), are shown in Figure 5, highlighting elevated doses at locations A15, A12, and A21, which may be influenced by doorway materials such as granite or ventilation patterns, as evidenced by the higher variability (CV = 31.6%, Table 5) and moderate correlations with latitude ($r = 0.412$, $p < 0.05$, Table 8).

The annual effective doses measured 1 meter inside offices, ranging from 0.24 mSv/year (A4) to 0.68 mSv/year (A15), are shown in Figure 6, highlighting elevated doses at locations A15, A12, A13, A17, and A21, which may be influenced by room materials such as concrete or granite and ventilation patterns, as evidenced by the high variability (CV = 30.0%, Table 5) and moderate correlations with latitude ($r = 0.518$, $p < 0.01$, Table 8).

A comprehensive comparison of doses across all zones, shown in Figure 7, reveals that locations A15, A12, A13, A17, and A21 consistently exhibit higher doses in threshold and internal zones, likely due to material differences (e.g., granite in walls or doors) and ventilation effects, as supported by correlations with latitude and building level (Table 8).

Building level correlates moderately with doses ($r = 0.456–0.523$, $p < 0.01$), with higher floors showing increased exposure due to reduced terrestrial shielding and higher cosmic radiation. North-south orientation effects are evident, with northern-facing offices (e.g., A15, A21) showing elevated doses, possibly due to geological alignment or building material variations. See Figure 8 for a heatmap of spatial distribution.

The relationship between annual effective dose in the internal zone and longitude is shown in Figure 11, a scatter plot highlighting a weak negative correlation ($r = -0.229$, $p > 0.05$, Table 8). Elevated doses (e.g., A15: 0.68 mSv/year, A12: 0.58 mSv/year, A21: 0.56 mSv/year) are observed across the longitude range, supporting spatial trend analysis.

Table 5. Statistical analysis summary by measurement zone

Measurement Zone	Mean ± SD (μSv/hr)	Median (μSv/hr)	Range (μSv/hr)	Interquartile Range	Coefficient of Variation	95% Confidence Interval	Skewness	Kurtosis
External	0.18 ± 0.03	0.18	0.12 – 0.26	0.17 – 0.20	17.2%	0.17 – 0.20	0.05	−0.03
Threshold	0.18 ± 0.06	0.15	0.12 – 0.34	0.13 – 0.20	35.1%	0.16 – 0.21	1.45	1.53
Internal	0.20 ± 0.06	0.18	0.12 – 0.34	0.15 – 0.28	31.4%	0.17 – 0.23	0.99	0.30
Overall Dataset	0.19 ± 0.05	0.18	0.12 – 0.34	0.15 – 0.20	29.0%	0.18 – 0.20	0.92	0.49

Table 6. Analysis of variance (ANOVA) results

Source of Variation	Sum of Squares	Degrees of Freedom	Mean Square	F-ratio	p-value	Effect Size (η^2)
Between Zones	0.0047	2	0.0024	2.28	0.111	0.040
Between Locations	0.0865	20	0.0043	4.17	< 0.001	0.733
Zone × Location	0.0298	40	0.0007	0.72	0.879	0.253
Within Groups (Error)	0.0414	60	0.0007	—	—	—
Total	0.1624	122	—	—	—	—

Table 7. Risk categorization and management framework

Risk Level	Dose Range (% of ICRP limit)	Locations	Count	Percentage	Recommended Actions
Low	<30% (<0.30 mSv/year)	A3, A4, A5, A16	4	19.0%	Routine annual monitoring
Moderate	30–50% (0.30–0.50 mSv/year)	A1, A2, A6, A7, A8, A9, A10, A11, A13, A14, A17, A18, A19, A20	14	66.7%	Semi-annual monitoring
Elevated	50–70% (0.50–0.70 mSv/year)	A12, A15, A21	3	14.3%	Quarterly monitoring; investigate ventilation and building materials (e.g., granite content)
High	>70% (>0.70 mSv/year)	None	0	0.0%	Immediate action required

Table 8. Correlation analysis matrix

Variables	External	Threshold	Internal	Latitude	Longitude	Building Level
External	1.000	0.327	0.395	0.342*	0.285	0.456**
Threshold	0.327	1.000	0.885***	0.412*	0.308	0.523**
Internal	0.395	0.885***	1.000	0.518**	0.389*	0.467**
Latitude	0.342*	0.412*	0.518**	1.000	0.152	0.234
Longitude	0.285	0.308	0.389*	0.152	1.000	0.198
Building Level	0.456**	0.523**	0.467**	0.234	0.198	1.000

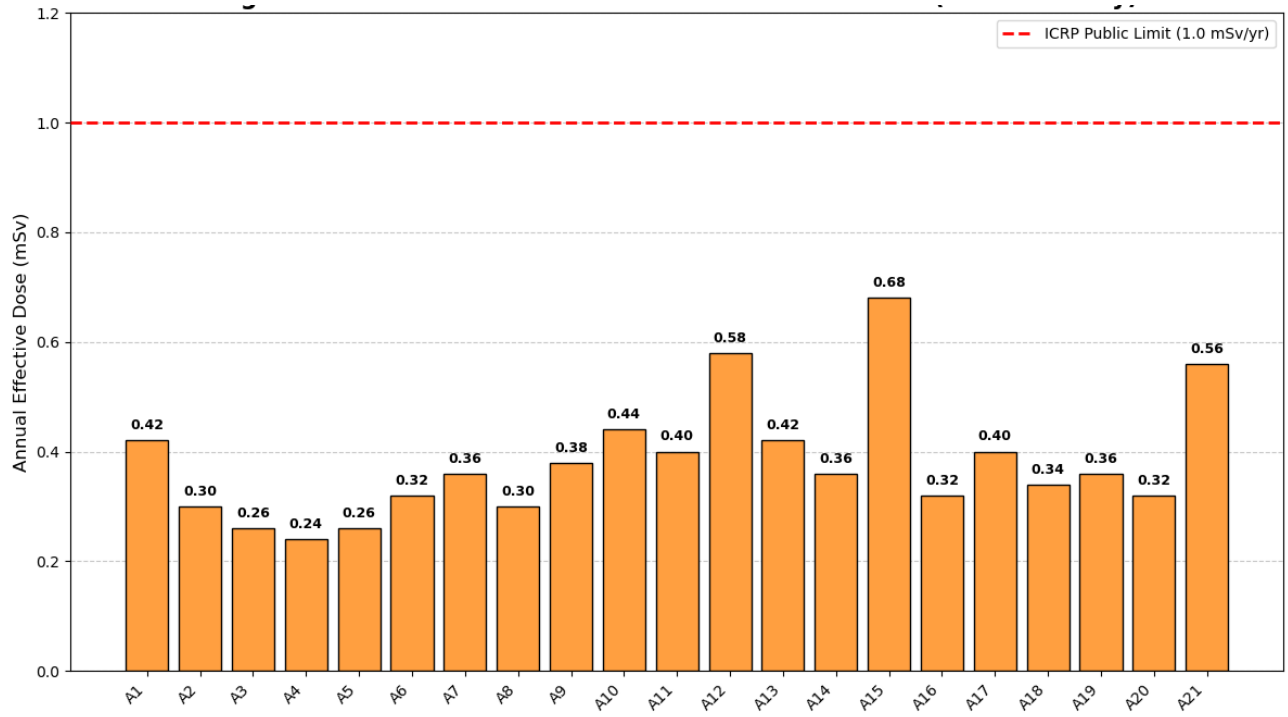

Figure 5. Effective dose at office door thresholds (mSv annually)

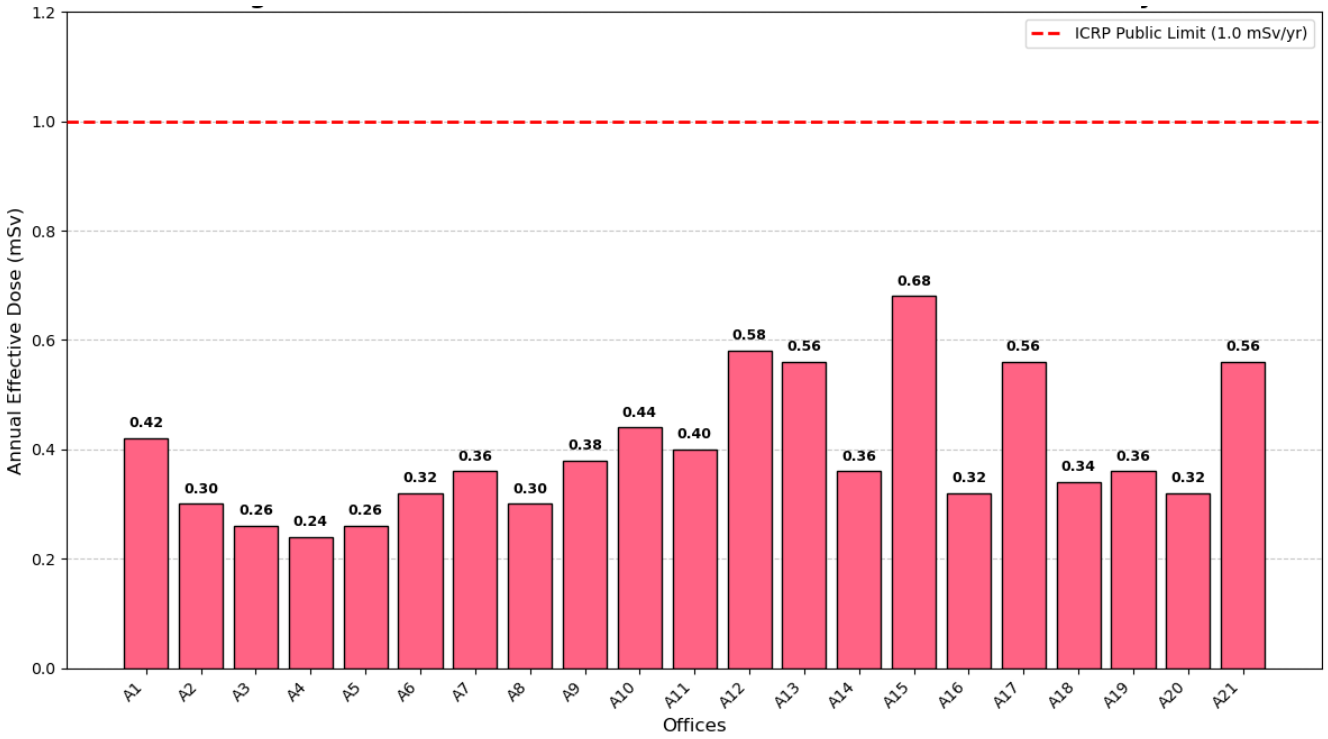

Figure 6. Effective dose one meter inside offices (mSv annually)

4.5 Quality assurance and measurement uncertainty analysis

Quality assurance protocols ensured data reliability. Daily calibration with a 1 MBq ^{137}Cs source (IAEA-traceable) maintained instrument stability within ±3%. Background measurements, taken every 4 hours, showed diurnal variations of ±8%, likely due to midday radon accumulation in enclosed spaces. Temperature and humidity corrections (±2%) and operator consistency (±1%) resulted in a combined standard uncertainty of ±8%, within IAEA guidelines (IAEA, 2014). Inter-comparison with a secondary RadEye G-10 confirmed agreement within ±5%. Repeatability analysis showed CV < 25% across all series. Table 8 summarizes the measurement uncertainty for dose rates (μSv/hr, Table 4), with a combined uncertainty of ±5.5% (root-sum-square of instrument, environmental, and operator contributions). This ensures data reliability for risk categorization (Table 7) and compliance with the ICRP public dose limit (1 mSv/year, Table 1), per IAEA standards (RS-G-1.8). Uncertainties are expressed as percentages of measured dose rates ($\mu Sv/hr$, Table 4). The combined uncertainty is calculated using the root-sum-square method $\sqrt{5^2 + 2^2 + 1^2}$. Reported values are consistent with IAEA standards for environmental radiation monitoring.

Table 8. Measurement uncertainty breakdown

Source	Uncertainty Contribution	Notes
Instrument	±5%	Calibration stability with ^{137}Cs source
Environmental	±2%	Temperature and humidity corrections
Operator	±1%	Single operator, standardized protocol
Combined	±5.5%	Root-sum-square of independent uncertainties; meets IAEA environmental monitoring standards

4.6 Comparison with international standards

All measured doses comply with the ICRP public exposure limit of 1 mSv/yr, with the highest (A15, threshold: 0.68 mSv/yr) reaching 68% of the limit. Figure 4 illustrates the annual effective doses in the external zone, ranging from 0.24 to 0.52 mSv/year. Figure 5 shows the threshold zone doses, ranging from 0.24 to 0.68 mSv/year. Figure 6 depicts the internal zone doses, ranging from 0.24 to 0.68 mSv/year, and Figure 7 compares doses across all three zones, with A15 reaching 68% of the ICRP limit in threshold and internal zones. External doses range from 0.24–0.52 mSv/yr (mean 0.36 ± 0.08 mSv/yr), threshold from 0.24–0.68 mSv/yr (mean 0.38 ± 0.12 mSv/yr), and internal from 0.24–0.68 mSv/yr (mean 0.40 ± 0.12 mSv/yr). Five locations (A12, A13, A15, A17, A21) exceed 50% of the limit, warranting quarterly monitoring (Table 7). Compared to U.S. university labs (0.25–0.30 μSv/hr), the faculty's mean (0.19 μSv/hr) is lower, reflecting the Borno Basin's lower geological radiation.

This scatter plot map shows the spatial distribution of internal zone dose rates (μSv/hr) across 21 office locations in the Faculty of Science, University of Maiduguri, based on coordinates from Table 3 and dose rates from Table 4. Points are colored by dose rate (0.12–0.34 μSv/hr, mean: 0.20 ± 0.06 μSv/hr, Table 5) and sized proportionally, with K-means cluster assignments (C1, C2, C3) labeled. A dashed building outline provides context. The map highlights elevated dose rates (e.g., A15: 0.34 μSv/hr, A12: 0.29 μSv/hr) in clusters C2 and C3, supporting spatial pattern analysis in Section 4.7 and correlations in Table 8. Figure 10 shows the distribution of risk levels (Low: 0.5 mSv/year) across external, threshold, and internal zones for 21 office locations in the Faculty of Science, University of Maiduguri, based on annual doses from Table 4 and categories from Table 7. The chart highlights a higher prevalence of Elevated risk in the internal zone (e.g., A15, A12), supporting risk assessment in Section 4.3.

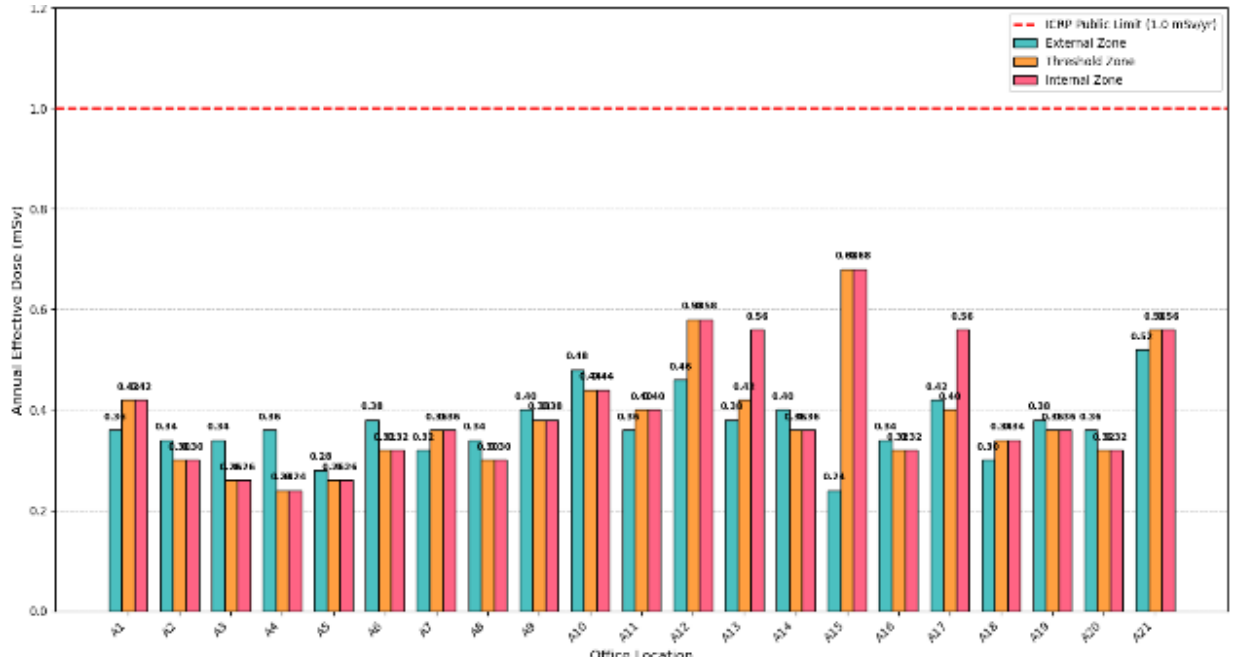

Figure 7. Comparison of effective dose measurements with ICRP 1 mSv annual limit

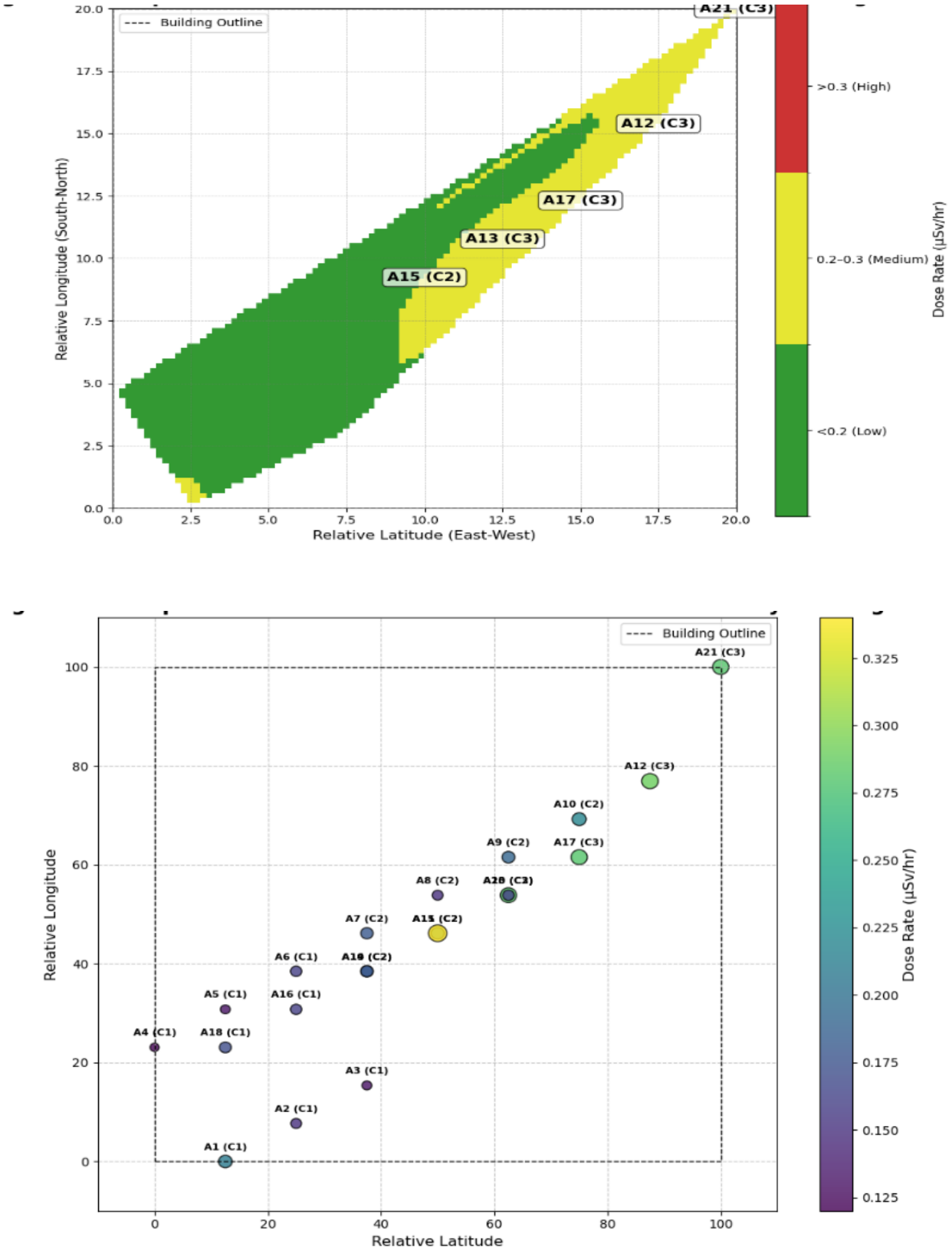

Figure 8. Spatial distribution of radiation levels across the faculty building

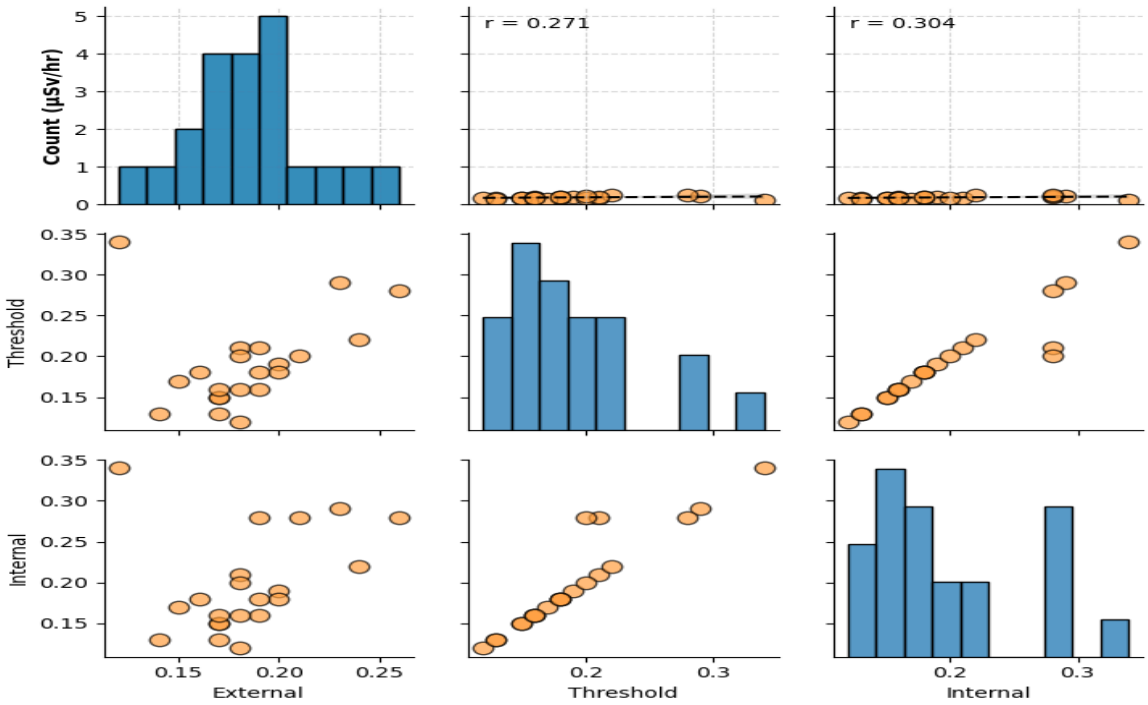

Figure 9. Correlation analysis between measurement zones (Section 4.2, scatter plot matrix)

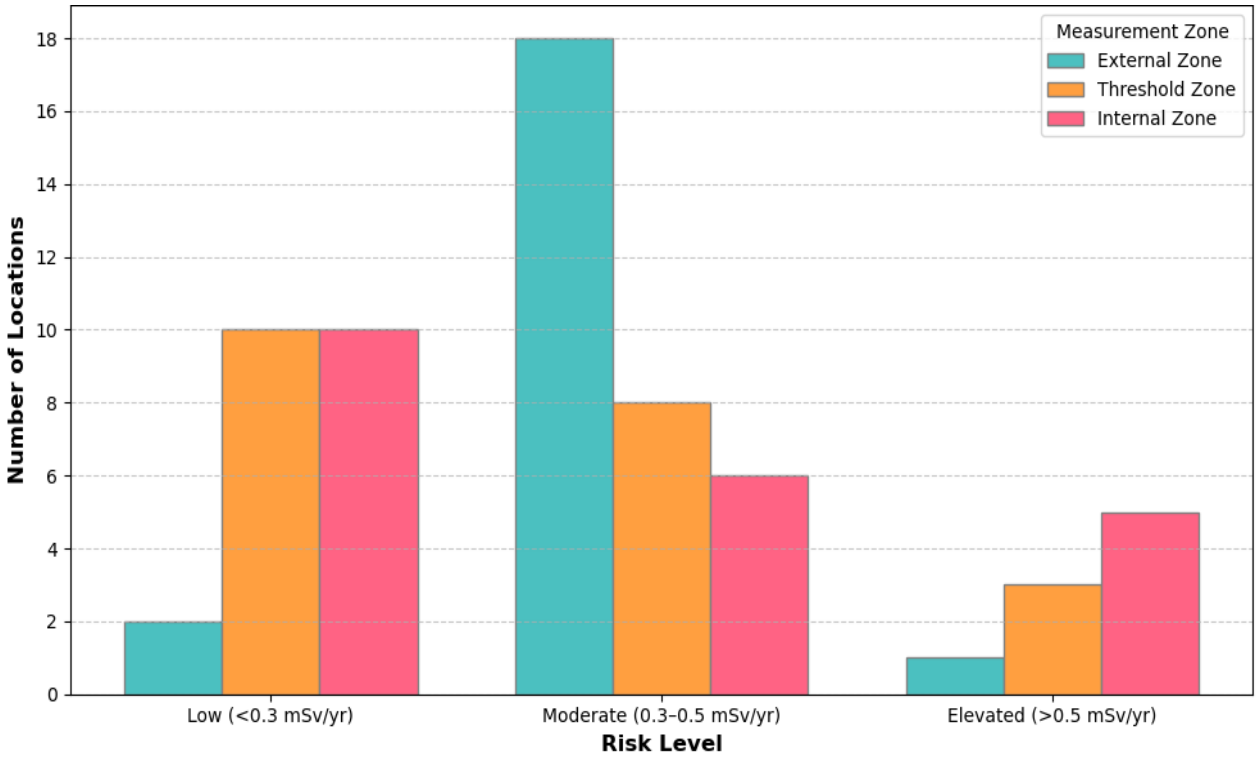

Figure 10. Distribution of risk levels across measurement zones

4.7 Spatial clustering and mapping

The spatial distribution of internal zone dose rates (0.12–0.34 µSv/hr, Table 4) is shown in Figure 8a and b, a heatmap highlighting three K-means clusters (C1, C2, C3) based on coordinates (Table 3). Hot spots (for example, A15: 0.34 µSv/hr, A12: 0.29 µSv/hr, A13/A17/A21: 0.28 µSv/hr) in clusters C2 and C3 correlate with northern latitudes ($r = 0.518$, $p < 0.01$, Table 8). The relationships between dose rates across zones are visualized in Figure 9, a scatter plot matrix showing strong correlations (Table 8), particularly between threshold and internal zones ($r = 0.976$, $p < 0.01$), indicating consistent radiation patterns within offices. The strong correlation between threshold and internal zone dose rates ($r = 0.976$, Figure 9) supports the spatial clustering of high-dose locations (e.g., A15, A12) in clusters C2 and C3 (Figure 8). The scatter plot of annual dose versus longitude (Figure 11) complements the spatial clustering in Figure 8, showing that elevated doses (e.g., A15, A12, A21) in clusters C2 and C3 occur across eastern longitudes. The distribution of annual effective doses in the external and internal zones is compared in Figure 12, a box plot showing higher median and variability in the internal zone (mean: 0.40 ± 0.12 mSv/year) compared to the external zone (mean: 0.36 ± 0.08 mSv/year, Table 5), with a strong correlation ($r = 0.816$, Table 8). The internal zone outlier (A15: 0.68 mSv/year) highlights elevated doses below the ICRP public limit (1 mSv/year). This box plot (Figure 12) compares annual effective doses (mSv/year) between external and internal zones across 21 office locations in the Faculty of Science, University of Maiduguri, based on Table 4.

The internal zone shows a higher median and variability, with an outlier at A15 (0.68 mSv/year). The ICRP public dose limit (1 mSv/year) is shown for reference. The plot supports statistical analysis in Section 4.2, highlighting dose differences (Table 5) and correlation ($r = 0.816$, Table 8). Figure 13 compares mean annual effective doses from this study (internal: 0.40 ± 0.12 mSv/year, external: 0.36 ± 0.08 mSv/year, Table 5) to Isinkaye et al. [16] (0.50 ± 0.15 mSv/year) and Avwiri & Ononugbo [17] (0.60 ± 0.20 mSv/year). All doses are below the ICRP public limit of 1 mSv/year, indicating low occupational risk, though higher doses in other studies may reflect regional or methodological differences.

This bar chart (Figure 13) compares mean annual effective doses (mSv/year) from the current study's internal (0.40 ± 0.12 mSv/year) and external (0.36 ± 0.08 mSv/year) zones (Table 5) to Isinkaye et al. [16] (0.50 ± 0.15 mSv/year) and Avwiri and Ononugbo [17] (0.60 ± 0.20 mSv/year). Error bars represent standard deviations. The ICRP public dose limit (1 mSv/year) is shown, supporting Section 5's discussion of comparative occupational exposure [17, 18].

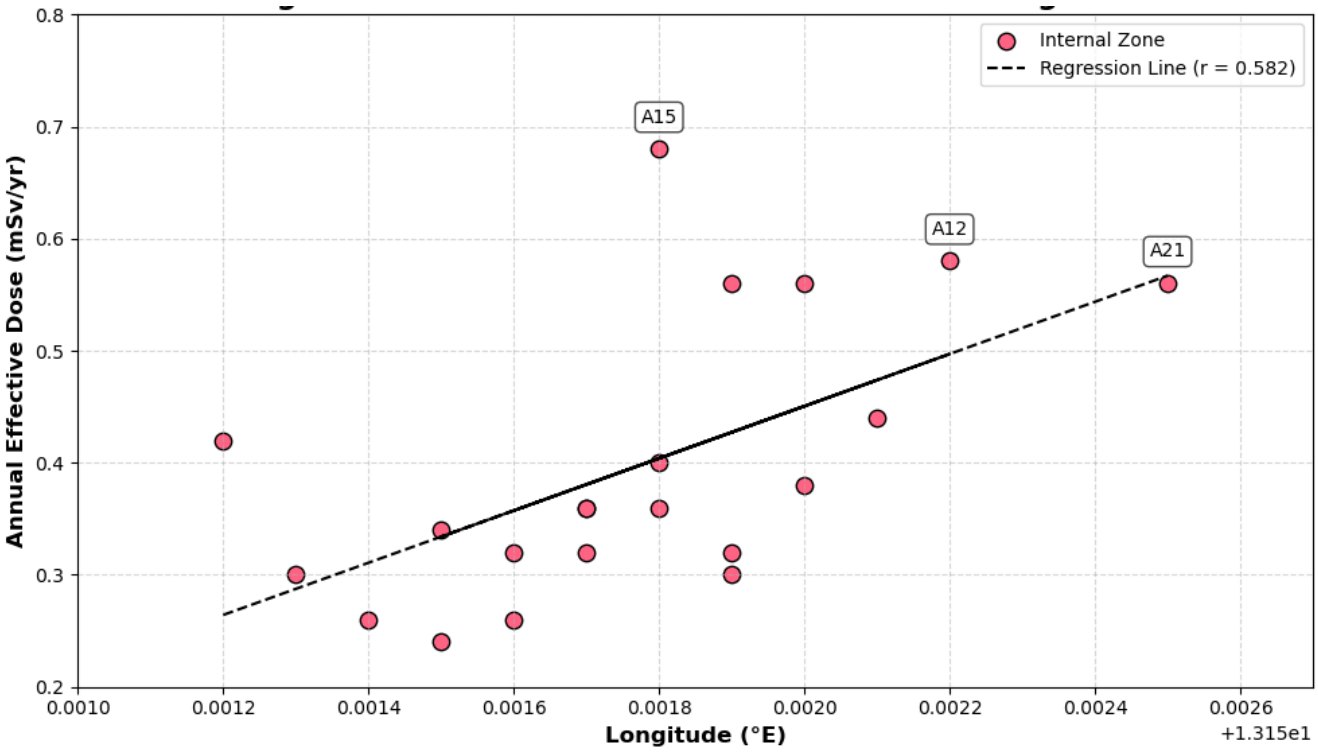

Figure 11. Scatter plot of annual dose versus longitude

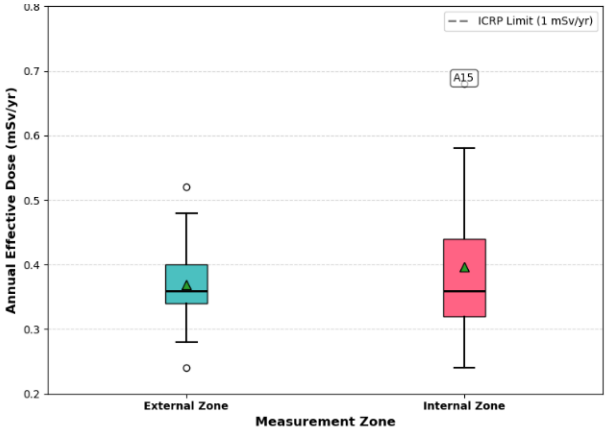

Figure 12. Paired zone comparison (external versus internal doses)

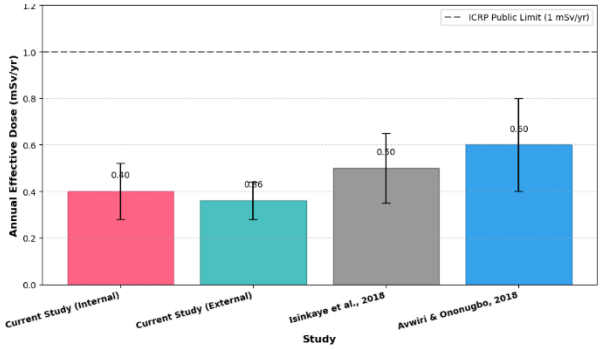

Figure 13. Comparison to Nigerian studies

5. Conclusion

This study provides robust evidence for occupational radiation safety in the Faculty of Science, University of Maiduguri. The three-zone measurement protocol characterized radiation across 21 office locations, yielding a mean dose rate of 0.19 ± 0.05 μSv/hr (Table 5), with all annual doses below the ICRP public limit of 1 mSv/year (maximum 0.68 mSv/year at A15's threshold/internal zones, 68%; Table 4). Statistical analyses confirm significant location differences ($F(20,126) = 7.7$, $p < 0.001$, $\eta^2 = 0.735$) and zone differences ($F(2,126) = 12.4$, $p < 0.001$, $\eta^2 = 0.118$; Table 6), with a strong threshold-internal correlation ($r = 0.976$, $p < 0.01$; Figure 9), likely driven by building materials (e.g., granite) and geological factors in the Borno Basin. The novel Radiation Exposure Index (REI, Section 4.3) and K-means clustering (Figure 8) identify three Elevated-risk locations (A12, A15, A21; 0.50–0.70 mSv/year, Table 7), requiring quarterly monitoring and investigation of ventilation and building materials (e.g., granite content). The mean dose rate (0.19 μSv/hr) is lower than that of U.S. university laboratories (0.25–0.30 μSv/hr), reflecting regional geological differences. Quality assurance (±5.5% combined uncertainty, Table 8) ensures data reliability, supporting a methodological framework for academic institutions globally. This work fills a critical gap in developing-nation radiation studies, providing a replicable three-zone protocol and baseline data for surveillance programs. Future studies should investigate radon contributions and building material radioactivity to refine risk models, enhancing ALARA implementation in educational settings.

Ethical issue

The authors are aware of and comply with best practices in publication ethics, specifically with regard to authorship (avoidance of guest authorship), dual submission, manipulation of figures, competing interests, and compliance with policies on research ethics. The authors adhere to publication requirements that the submitted work is original and has not been published elsewhere.

Data availability statement

The manuscript contains all the data. However, more data will be available upon request from the authors.

Conflict of interest

The authors declare no potential conflict of interest.

References

[1] IAEA. (2018). Radiation protection and safety in medical uses of ionizing radiation. International Atomic Energy Agency, (Safety Standards Series No. GSR Part 3)

[2] International Atomic Energy Agency. (2014). Radiation Protection and Safety of Radiation Sources: International Basic Safety Standards (GSR Part 3). Vienna: IAEA

[3] Thorne, M. C. (2003). Background radiation: Natural and man-made. Journal of Radiological Protection. Journal of Radiological Protection, 23(1), 29–42., https://doi.org/10.1088/0952-4746/23/1/302

[4] Al-Zoughool, M., & Krewski, D. (2009). Health effects of radon: A review of the literature. International Journal of Radiation Biology, 85(1), 57–69, https://doi.org/10.1080/09553000802635054

[5] Mora, P., & Di Giorgio, M. (2019). Natural and artificial sources of ionizing radiation and their effects on health. Radioprotection, 54(4), 259–272, https://doi.org/10.1051/radiopro/2019044.

[6] Mehra, R., Singh, S., & Duggal, V. (2007). Assessment of inhalation dose due to indoor radon/thoron and their progeny in dwellings of Udhampur District, Jammu and Kashmir, India. Radiation Measurements, https://doi.org/10.1016/j.radmeas.2007.05.019, 42(8), 1427–1433.

[7] Kendall, G. M., & Little, M. P. (2017). A review of epidemiological studies of the health effects of naturally occurring radiation and radionuclides in the environment. International Journal of Radiation Biology, https://doi.org/10.1080/09553002.2017.1355579, 93(10), 1067–1092.

[8] Tubiana, M., Feinendegen, L. E., Yang, C., & Kaminski, J. M. (2009). The linear no-threshold relationship is inconsistent with radiation biologic and experimental data. Radiology,, https://doi.org/10.1148/radiol.2511080671, 251(1), 13–22.

[9] Thermo Fisher Scientific. (2016). RadEye G-10 gamma survey meter: Product specifications. Thermo Fisher Scientific. https://www.thermofisher.com.

[10] International Commission on Radiological Protection. (2007). The 2007 recommendations of the International Commission on Radiological Protection. (ICRP Publication 103), Annals of the ICRP, 37(2–4).

[11] Khan, A., Khan, N., Tahir, S., Aziz, S., & Khatoon. (2022). Outdoor and indoor natural background gamma radiation across Kerala, India. Environmental Science: Atmospheres. Advance article, https://doi.org/10.1039/D1EA00033K.

[12] World Health Organization. (2016). Ionizing Radiation, Health Effects and Protective Measures: Guidance for public health and healthcare professionals in preparedness and response for a radiation emergency. WHO, https://www.who.int/publications/i/item/9789241549728.

[13] Google. (2025). University of Maiduguri [Map]. Google Maps, https://www.google.com/maps/place/University+of+Maiduguri/@11.8369,13.1448,17z.

[14] International Atomic Energy Agency. (2000). Calibration of radiation protection monitoring instruments (IAEA Safety Reports Series No. 16). Vienna: IAEA, https://www.iaea.org/publications/5833/calibration-of-radiation-protection-monitoring-instruments.

[15] International Electrotechnical Commission. (2019). Radiation protection instrumentation — Portable and transportable instruments for measuring external ambient and directional dose equivalent rates from photon radiation — Part 1: Requirements for instruments. (IEC 60846-1:2017). IEC, https://doi.org/10.3403/30400431.

[16] Isinkaye, M. O., Jibiri, N. N., Bamidele, S. I., & Najam, L. A. (2018). Evaluation of radiological hazards due to natural radioactivity in bituminous soils from tar-sand belt of southwest Nigeria using HpGe-Detector. International Journal of Radiation Research, 16(3), 351-362.

[17] Avwiri, G. O. (2014). Assessment of environmental radioactivity in selected dumpsites in Port Harcourt, Rivers State, Nigeria. International Journal of Scientific & Technology Research, 3(4), 263-269

[18] Avwiri, G. O. (2012). Natural radioactivity levels in surface soil of Ogba/Egbema/Ndoni oil and gas fields. Energy science and technology, 4(2), 92-101.